Structure and Properties of Tris(quinoxaline-2,3-dithiolato)molybdate(IV)†

Stephen Boyde and C. David Garner *
The Chemistry Department, Manchester University, Manchester M13 9PL
John H. Enemark * **and Richard B. Ortega**
Department of Chemistry, University of Arizona, Tucson, Arizona 85721, U.S.A.

The synthesis, crystal structure, spectroscopic and electrochemical properties of tris(quinoxaline-2,3-dithiolato)molybdate(IV), $[Mo(qdt)_3]^{2-}$, are reported. $[PPh_4]_2[Mo(qdt)_3]\cdot H_2O$ crystallizes in the space group $P2_1/c$, with $a = 20.150(20)$, $b = 14.014(5)$, $c = 23.530(20)$ Å, $\beta = 104.34(8)°$, and $Z = 4$. The anion has an essentially trigonal prismatic MoS_6 core with Mo–S (average) 2.393(10) Å. $[Mo(qdt)_3]^{2-}$ undergoes reversible protonation on the ligand nitrogen atoms and the triply protonated species, formulated as $[Mo(Hqdt)_3]^+$, has been isolated and characterized as its chloride salt. Cyclic voltammetry indicates that $[Mo(qdt)_3]^{2-}$ undergoes one-electron reduction and oxidation processes. The oxidation product, $[Mo(qdt)_3]^-$ (e.s.r. parameters $g = 2.002$, $\bar{A} = 32.9$), can be generated in solution by chemical oxidation.

Stimulated by the recent suggestion that molybdenum in the molybdenum hydroxylase enzymes may be bound to an unsaturated 1,2-dithiolate group,[1] we have been further investigating the chemistry of molybdenum complexes of such ligands (*i.e.* molybdenum dithioles).[2] The ligand quinoxaline-2,3-dithiolate (qdt) appeared to be particularly interesting, as its complexes with other metals have been prepared and reported to undergo reversible protonation of the ligand nitrogen atoms[3] as well as the reversible electron-transfer reactions typical of metal dithioles.[4] Such behaviour could have relevance to the reactivity of the molybdopterin which constitutes the molybdenum cofactor of these hydroxylase enzymes.[1] Complexes of qdt with Zn, Cu, Ni, Pd, and Pt[4] and Co and Fe[5,6] have been reported but the only previous account of complex formation between molybdenum and qdt was an e.s.r. study of species present in solution in which no complexes were isolated.[7]

Herein we report the synthesis, spectroscopic and electrochemical properties of $[Mo(qdt)_3]^{2-}$ and the crystal structure of $[PPh_4]_2[Mo(qdt)_3]\cdot H_2O$, together with the preparation of the triply protonated complex formulated as $[Mo(Hqdt)_3]^+$.

Experimental

Materials and Methods.—The compounds H_2qdt[8] and $[MoO_2(acac)_2]$[9] (acac = acetylacetonate) were prepared by literature methods. The complexes prepared in this study are air- and moisture-stable, except for $[Mo(qdt)_3]^-$, which was manipulated in dry, degassed solvents under a purified dinitrogen atmosphere.

Instrumentation and Analyses.—Chemical analyses were performed by the University of Manchester Microanalytical Laboratory. Spectra were recorded on the following instruments: i.r., Perkin-Elmer 577; u.v.–visible, Shimadzu UV-260; e.s.r., Varian 112; ^1H and ^{13}C n.m.r., Varian SC300. Cyclic voltammograms were obtained using an EG & G model 175 waveform generator and model 173 potentiostat.

Syntheses.—$[PPh_4]_2[Mo(qdt)_3]\cdot H_2O$. The ligand H_2qdt (2 g, 10.3 mmol) was added to a stirred suspension of $[MoO_2(acac)_2]$ (1.2 g, 3.4 mmol) in 98% H_2SO_4 (40 cm^3). After 10 min, the bottle-green solution was poured into H_2O (500 cm^3), whence a dark green powder precipitated. This was separated by filtration and redissolved in MeOH (50 cm^3) containing NaOH (1 g, 25 mmol), to give a purple solution which was filtered into a solution of $[PPh_4]Br$ (2.9 g, 6.9 mmol) in MeOH (10 cm^3). After standing for 3 h, the mixture was filtered to isolate the purple, needle-like crystals of $[PPh_4]_2[Mo(qdt)_3]\cdot H_2O$. Recrystallization from MeCN gave large, rectangular, purple crystals. Yield: 2.65 g, 55% (Found: C, 63.1; H, 3.8; Mo, 7.5; N, 6.3; P, 4.4; S, 13.3. $C_{72}H_{54}MoN_6OP_2S_6$ requires C, 63.1; H, 4.0; Mo, 7.0; N, 6.1; P, 4.5; S, 14.0 %).

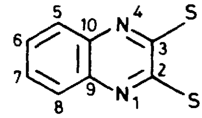

qdt

Figure 1. Formula of the qdt anion

$[NEt_4]_2[Mo(qdt)_3]\cdot 3H_2O$. This compound was synthesized by the same method as $[PPh_4]_2[Mo(qdt)_3]\cdot H_2O$, using $[NEt_4]Br$ in place of $[PPh_4]Br$. Yield: 50% (Found: C, 49.0; H, 5.8; Mo, 9.6; N, 11.5; S, 19.3. $C_{40}H_{58}MoN_8O_3S_6$ requires C, 48.8; H, 5.7; Mo, 9.7; N, 11.4; S, 19.5%).

$[Mo(Hqdt)_3]Cl$. The compound $[PPh_4]_2[Mo(qdt)_3]\cdot H_2O$ (0.3 g, 2.14 mmol) was dissolved in MeCN (40 cm^3) and acidified by the addition of HCl (36%, 2 cm^3) in MeCN (20 cm^3). The solution changed colour from purple to blue-green and the finely divided turquoise precipitate of $[Mo(Hqdt)_3]Cl$ was collected by filtration. Yield: 0.15 g, 97% (Found: C, 40.0; H, 2.3; Cl, 5.3; Mo, 14.0; N, 11.5; S, 26.6. $C_{24}H_{15}ClMoN_6S_6$ requires C, 40.5; H, 2.1; Cl, 5.0; Mo, 13.5; N, 11.8; S, 27.1%).

Crystal Structure Determination.—Crystals of $[PPh_4]_2[Mo(qdt)_3]\cdot H_2O$ suitable for structure determination by *X*-ray diffraction were obtained by slow evaporation in air of a MeCN solution.

Preliminary examination and data collection were accomplished with Mo-K_α radiation on a Nicolet/Syntex $P2_1$ computer-controlled diffractometer, equipped with a graphite-crystal, incident beam monochromator. Cell constants and an orientation matrix for data collection were obtained from least-squares refinement, using the setting angles of 25 reflections in the range $12 < 2\theta < 26°$. The cell parameters and calculated

---

† *Supplementary data available:* see Instructions for Authors, *J. Chem. Soc., Dalton Trans.*, 1987, Issue 1, pp. xvii—xx.

Table 1. Experimental details for the *X*-ray crystallographic study of $[PPh_4]_2[Mo(qdt)_3]\cdot H_2O$

Crystal data

$C_{72}H_{52}MoN_6P_2S_6\cdot H_2O$ $M = 1\,369.5$ $F(000) = 2\,816$
Crystal dimensions 0.80 × 0.75 × 0.35 mm
Peak width at half-height 0.25°
Mo-K_α radiation ($\lambda = 0.710\,73$ Å)
Monoclinic, space group $P2_1/c$
$a = 20.150(20)$ Å $b = 14.014(5)$ Å $c = 23.530(20)$ Å
$\beta = 104.34(8)°$ $U = 6\,437.4$ Å^3 $Z = 4$
$D_c = 1.42$ g cm^{-3} $\mu = 4.8$ cm^{-1} $T = 23(1)$ °C

Intensity measurements

Instrument	Nicolet/Syntex $P2_1$ diffractometer running locally modified $P3$ software
Monochromator	Graphite crystal, incident beam
Crystal–detector distance	21 cm
Incident beam collimator	0.75 mm diameter
Scan type	omega
Scan rate	1.5—15.0° min^{-1} (in omega)
Scan width	2.8°
Maximum 2θ	45.0°
Number of reflections measured	9 089 total, 8 391 unique
Corrections	Lorentz-polarization Empirical absorption correction based on psi scans; relative transmission coefficients 0.715—0.845 Reflection averaging (agreement on *I* for 318 observed and accepted reflections, 4.3%)

Structure refinement

Refinement	Full matrix least-squares
Minimization function	$\Sigma w(\lvert F_o\rvert - \lvert F_c\rvert)^2$
Least-squares weights	$4F_o^2/\sigma^2(F_o^2)$
Anomalous dispersion	All non-hydrogen atoms
Reflections included	6 025 with $F_o^2 > 2.0\sigma(F_o^2)$
Parameters refined	765
Unweighted agreement factor	0.060
Weighted agreement factor	0.067
E.s.d. of observation of unit weight	2.84
Convergence, largest shift	0.30σ
Highest peak in final difference Fourier map	0.62 e Å^{-3}

volume (Table 1) were based on a constrained refinement in the monoclinic crystal system. As a check on crystal quality, omega scans of several intense reflections were measured; the width at half-height was 0.25°, indicating good crystal quality. From the systematic absences of $h0l, l = 2n + 1$ and $0k0, k = 2n + 1$, the space group was determined to be $P2_1/c$ (no. 14).

Fixed background counts were made at the scan extremes, such that the ratio of peak counting time to background counting time was 2:1. As a check on crystal and electronic stability, two representative reflections were measured every 98 reflections. The intensities of the standards remained constant within experimental error throughout the experiment, therefore, no decay correction was applied. Details of data collection and corrections applied to the data are summarized in Table 1.

The structure was solved using the Patterson heavy-atom method which revealed the position of the Mo atom. The remaining atoms were located in succeeding difference Fourier syntheses. Hydrogen atoms were included in the structure factor calculations at their calculated positions but not refined. The hydrogen atoms on the water molecule were not located and were omitted from the calculations. The details of the refinement of the structure are given in Table 1.

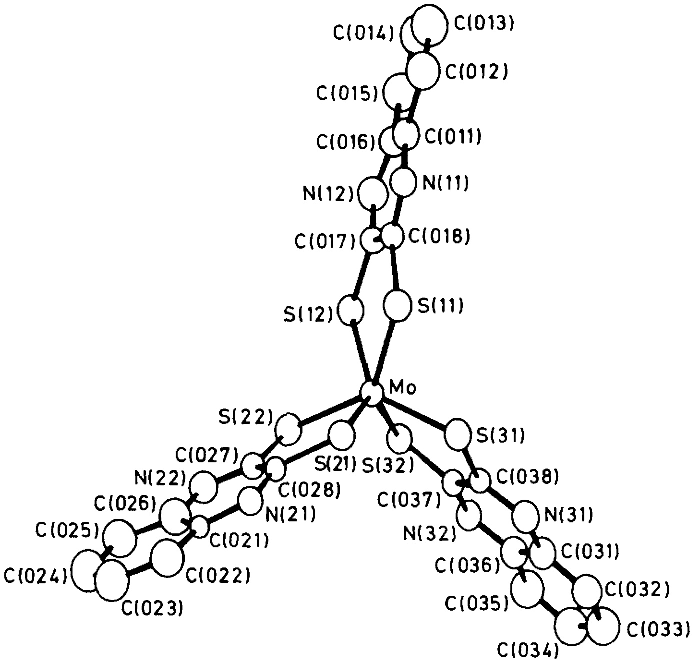

Figure 2. The structure of $[Mo(qdt)_3]^{2-}$ showing the crystallographic atom numbering

The standard deviation on intensities, $\sigma(F_o^2)$, is defined by $[\sigma^2(I) + (pI)^2]^{\frac{1}{2}}$, where $\sigma(I)$ is the standard deviation on *I* due to counting statistics and the parameter *p* is a factor introduced to downweight intense reflections. Here *p* was set to 0.03.

Scattering factors were taken from Cromer and Waber.[10] Anomalous dispersion effects were included in F_c;[11] the values for f' and f'' were those of Cromer and Waber.[12]

Plots of $\Sigma w(\lvert F_o\rvert - \lvert F_c\rvert)^2$ *vs.* $\lvert F_o\rvert$, reflection order in data collection, $\sin\theta/\lambda$, and various classes of indices showed no unusual trends. All calculations were performed on a PDP-11/34a computer using SDP-Plus.[13] The final refined atomic co-ordinates are presented in Table 2.

Results and Discussion

The free ligand H_2qdt is only sparingly soluble in most organic solvents. It exists as the dithioamide form rather than the dithiol[14] and the thioamide protons are less acidic than 'normal' thiol protons. Consequently, extremely basic conditions are required to deprotonate the ligand and render it soluble in the organic solvents which would be the preferred media for synthesis of metal complexes.[4] The synthetic route to $[Mo(qdt)_3]^{2-}$ described above is based on that of Gilbert and Sandell[15] for the preparation of tris(toluene-3,4-dithiolato)-molybdenum(VI). The strongly acidic medium appears to allow facile replacement of terminal oxo groups, $[MoO_4]^{2-}$ or $[MoO_2(acac)_2]$, *via* a protonation–dehydration mechanism.

Crystal Structure of $[PPh_4]_2[Mo(qdt)_3]\cdot H_2O$.—A perspective view of the structure and the numbering scheme for the anion $[Mo(qdt)_3]^{2-}$ are shown in Figure 2; selected interatomic distances and interbond angles are listed in Tables 3 and 4, respectively. The co-ordination geometry of the MoS_6 core is nearly perfectly trigonal prismatic. The average Mo–S distance is 2.393(10) Å, the average intra-ligand S···S distance is 3.127(6) Å, and the average inter-ligand S···S separation is 3.142(20) Å.

Table 2. Positional parameters with estimated standard deviations for $[PPh_4]_2[Mo(qdt)_3]\cdot H_2O$

Atom	X/a	Y/b	Z/c
Mo	0.757 22(3)	0.097 15(4)	0.208 93(2)
S(11)	0.814 08(9)	−0.053 4(1)	0.212 43(8)
S(12)	0.679 72(9)	0.022 4(1)	0.127 11(8)
S(21)	0.874 18(9)	0.150 8(1)	0.236 21(8)
S(22)	0.746 47(9)	0.228 1(1)	0.143 20(8)
S(31)	0.777 92(9)	0.071 0(1)	0.312 06(7)
S(32)	0.652 31(9)	0.161 4(1)	0.223 65(7)
P(1)	0.909 46(9)	−0.164 6(1)	−0.041 23(8)
P(2)	0.616 8(1)	0.543 4(1)	0.275 44(8)
O(W)	0.950 3(3)	−0.200 6(5)	0.176 3(2)
N(11)	0.786 4(3)	−0.216 6(4)	0.156 7(2)
N(12)	0.657 1(3)	−0.155 3(4)	0.089 6(3)
N(21)	0.944 0(3)	0.293 9(4)	0.205 2(2)
N(22)	0.830 1(3)	0.356 1(4)	0.116 2(2)
N(31)	0.723 5(3)	0.131 3(4)	0.396 8(2)
N(32)	0.608 9(3)	0.214 8(4)	0.316 3(2)
C(011)	0.740 8(4)	−0.278 4(5)	0.121 0(3)
C(012)	0.761 8(5)	−0.374 1(5)	0.117 4(3)
C(013)	0.714 7(6)	−0.438 5(6)	0.086 2(4)
C(014)	0.649 1(5)	−0.408 8(6)	0.055 9(4)
C(015)	0.631 0(4)	−0.316 1(6)	0.058 3(4)
C(016)	0.676 2(4)	−0.248 9(5)	0.090 2(3)
C(017)	0.700 6(3)	−0.096 5(5)	0.124 9(3)
C(018)	0.764 8(3)	−0.130 6(5)	0.160 4(3)
C(021)	0.949 6(3)	0.368 3(5)	0.169 8(3)
C(022)	1.012 7(4)	0.416 2(6)	0.176 9(3)
C(023)	1.021 2(4)	0.488 7(6)	0.141 6(4)
C(024)	0.963 5(5)	0.520 3(6)	0.096 6(4)
C(025)	0.903 0(5)	0.475 7(6)	0.089 4(4)
C(026)	0.893 6(4)	0.398 4(5)	0.125 5(3)
C(027)	0.825 6(3)	0.283 9(5)	0.150 7(3)
C(028)	0.883 6(3)	0.249 6(5)	0.194 7(3)
C(031)	0.673 1(3)	0.180 7(5)	0.416 2(3)
C(032)	0.679 3(4)	0.190 3(6)	0.475 6(3)
C(033)	0.629 9(4)	0.237 9(7)	0.495 6(3)
C(034)	0.575 2(4)	0.279 8(7)	0.456 8(4)
C(035)	0.568 1(4)	0.271 4(6)	0.397 3(3)
C(036)	0.617 7(3)	0.221 8(5)	0.376 0(3)
C(037)	0.656 9(3)	0.169 6(5)	0.298 5(3)
C(038)	0.715 6(3)	0.127 1(5)	0.339 0(3)
C(041)	0.991 1(4)	−0.208 5(5)	0.000 8(3)
C(042)	1.038 8(4)	−0.238 2(7)	−0.026 2(3)
C(043)	1.098 0(4)	−0.279 8(7)	0.004 7(4)
C(044)	1.108 6(4)	−0.296 7(6)	0.063 6(4)
C(045)	1.061 4(4)	−0.268 0(6)	0.091 5(3)
C(046)	1.001 2(4)	−0.225 3(6)	0.060 6(3)
C(051)	0.876 6(3)	−0.062 6(5)	−0.010 8(3)
C(052)	0.843 1(4)	0.007 7(5)	−0.049 4(3)
C(053)	0.809 5(5)	0.079 5(6)	−0.028 0(4)
C(054)	0.809 6(4)	0.084 5(6)	0.029 9(4)
C(055)	0.844 3(4)	0.016 4(6)	0.068 1(3)
C(056)	0.876 2(4)	−0.057 4(6)	0.047 3(3)
C(061)	0.848 3(4)	−0.258 0(5)	−0.045 0(3)
C(062)	0.866 7(4)	−0.352 4(6)	−0.052 9(3)
C(063)	0.816 2(5)	−0.424 7(5)	−0.058 0(4)
C(064)	0.753 3(5)	−0.404 1(6)	−0.054 1(4)
C(065)	0.734 9(4)	−0.312 2(7)	−0.044 8(4)
C(066)	0.781 9(4)	−0.238 1(5)	−0.041 2(4)
C(071)	0.918 5(4)	−0.136 7(6)	−0.113 3(3)
C(072)	0.885 6(4)	−0.188 8(5)	−0.161 3(3)
C(073)	0.895 9(4)	−0.169 0(7)	−0.216 3(3)
C(074)	0.942 3(5)	−0.106 6(8)	−0.221 4(3)
C(075)	0.975 6(5)	−0.047 2(8)	−0.174 6(4)
C(076)	0.963 7(4)	−0.064 7(6)	−0.120 3(3)
C(081)	0.696 2(3)	0.481 5(5)	0.281 3(3)
C(082)	0.714 1(4)	0.405 4(5)	0.317 8(3)
C(083)	0.774 7(4)	0.357 2(6)	0.319 4(3)
C(084)	0.815 5(4)	0.384 9(6)	0.285 5(3)
C(085)	0.797 8(4)	0.459 3(7)	0.249 2(4)
C(086)	0.737 4(5)	0.508 3(7)	0.247 1(4)
C(091)	0.592 9(3)	0.537 0(6)	0.343 7(3)
C(092)	0.525 7(4)	0.536 1(8)	0.347 1(4)
C(093)	0.510 6(4)	0.544 6(9)	0.402 3(4)
C(094)	0.561 5(5)	0.549 1(8)	0.451 6(4)
C(095)	0.627 0(5)	0.550 1(8)	0.449 4(4)
C(096)	0.644 4(4)	0.543 3(7)	0.395 4(4)
C(101)	0.554 6(4)	0.490 6(6)	0.216 0(3)
C(102a)	0.492 4(7)	0.531(1)	0.196 5(6)
C(102b)	0.520 1(9)	0.544(1)	0.164 5(8)
C(103a)	0.445 9(8)	0.487(1)	0.150 1(7)
C(103b)	0.479(1)	0.497(2)	0.115 0(9)
C(104)	0.465 2(5)	0.401 0(8)	0.123 0(5)
C(105a)	0.532 6(9)	0.360(1)	0.145 0(7)
C(105b)	0.500 4(9)	0.345(1)	0.170 5(7)
C(106a)	0.574 7(7)	0.403(1)	0.193 4(6)
C(106b)	0.540 5(9)	0.392(1)	0.216 6(7)
C(111)	0.627 1(4)	0.668 4(5)	0.261 2(3)
C(112a)	0.599 1(7)	0.711(1)	0.208 6(6)
C(112b)	0.571 4(9)	0.723(1)	0.250 6(8)
C(113a)	0.607 3(7)	0.806(1)	0.200 0(6)
C(113b)	0.577(1)	0.826(1)	0.246 1(8)
C(114)	0.644 2(5)	0.861 6(7)	0.249 8(4)
C(115a)	0.675 9(8)	0.823(1)	0.295 4(7)
C(115b)	0.699 7(8)	0.810(1)	0.276 3(7)
C(116a)	0.666 3(8)	0.724(1)	0.305 1(7)
C(116b)	0.688 8(8)	0.710(1)	0.277 7(7)

The three approximately planar qdt ligands show small but crystallographically significant conformational differences.* Ligand 1 is twisted, so that atom S(11) is 0.23 Å out of the least-squares plane of the $S_2C_8N_2$ fragment, ligand 2 has all atoms within 0.08 Å of its least-squares plane, and in ligand 3 the largest deviation of an atom from the least-squares plane is only 0.04 Å. The three molybdadithiole (MoS_2C_2) rings also show small but significant conformational differences. Each ring can be described as an envelope folded along the S $\cdots$ S vector. The angles between the appropriate MoS_2 planes and the mean ligand least-squares planes described above are 12°, 3°, and 12°, respectively. Similar puckering of the molybdadithiolene rings has previously been observed for the neutral, trigonal prismatic complexes, tris(benzene-1,2-dithiolato)molybdenum(VI), $[Mo(bzdt)_3]$,[16] and tris(ethene-1,2-dithiolato)molybdenum(VI), $[Mo(edt)_3]$.[17]

The dianionic dithiole complex tris(maleonitriledithiolato)-molybdate(IV), $[Mo(mnt)_3]^{2-}$,[18,19] adopts a structure intermediate between octahedral and trigonal prismatic geometry and it has been suggested[19] that this difference in structure between $[Mo(mnt)_3]^{2-}$ and *e.g.* $[Mo(bzdt)_3]$ reflects the difference in the formal oxidation state of Mo in the two complexes, *i.e.* an increase in the number of valence electrons about the Mo atom favours octahedral over trigonal prismatic geometry, both because of metal–ligand and inter-ligand interactions. On this basis, it might be anticipated that $[Mo(qdt)_3]^{2-}$, a formally Mo^{IV} complex, would adopt a

---

* The partially refined structure of $[PPh_4]_2[Mo(qdt)_3]\cdot H_2O$ has been reported previously (S. Boyde, C. D. Garner, J. H. Enemark, and R. B. Ortega, *Polyhedron*, 1986, **5**, 377), in which the ligands were described as planar.

Table 3. Selected bond lengths (Å)* for the anion of $[PPh_4]_2[Mo(qdt)_3]\cdot H_2O$

Mo–S(11)	2.393(1)	S(11)–C(018)	1.748(4)	C(011)–C(012)	1.416(6)	C(021)–C(026)	1.397(6)
Mo–S(12)	2.399(1)	S(12)–C(017)	1.723(4)	C(011)–C(016)	1.387(6)	C(022)–C(023)	1.350(7)
Mo–S(21)	2.405(1)	S(21)–C(028)	1.732(4)	C(012)–C(013)	1.381(8)	C(023)–C(024)	1.434(7)
Mo–S(22)	2.375(1)	S(22)–C(027)	1.745(4)	C(013)–C(014)	1.400(9)	C(024)–C(025)	1.343(7)
Mo–S(31)	2.387(1)	S(31)–C(038)	1.729(4)	C(014)–C(015)	1.354(8)	C(025)–C(026)	1.418(6)
Mo–S(32)	2.400(1)	S(32)–C(037)	1.745(4)	C(015)–C(016)	1.394(7)	C(027)–C(028)	1.440(5)
				C(017)–C(018)	1.436(6)	C(031)–C(032)	1.380(6)
average Mo–S	2.393(10)	average S–C	1.737(9)	C(021)–C(022)	1.412(6)	C(031)–C(036)	1.396(6)
						C(032)–C(033)	1.374(7)
N(11)–C(011)	1.384(6)	N(21)–C(021)	1.357(5)	N(31)–C(031)	1.395(5)	C(033)–C(034)	1.376(8)
N(11)–C(018)	1.291(5)	N(21)–C(028)	1.334(5)	N(31)–C(038)	1.330(5)	C(034)–C(035)	1.377(7)
N(12)–C(016)	1.365(6)	N(22)–C(026)	1.378(5)	N(32)–C(036)	1.374(5)	C(035)–C(036)	1.409(6)
N(12)–C(017)	1.333(5)	N(22)–C(027)	1.315(5)	N(32)–C(037)	1.308(5)	C(037)–C(038)	1.450(5)

* The number in parentheses is the estimated standard deviation in the least significant digit.

Table 4. Selected interbond angles (°)* for the anion of $[PPh_4]_2[Mo(qdt)_3]\cdot H_2O$

S(11)–Mo–S(12)	81.58(4)	Mo–S(11)–C(018)	109.7(2)	C(014)–C(015)–C(016)	121.6(6)	S(22)–C(027)–C(028)	118.8(3)
S(11)–Mo–S(21)	80.62(4)	Mo–S(12)–C(017)	109.3(2)	N(12)–C(016)–C(011)	121.1(4)	N(22)–C(027)–C(028)	122.2(4)
S(11)–Mo–S(31)	82.42(4)	Mo–S(21)–C(028)	109.7(2)	N(12)–C(016)–C(015)	119.9(5)	S(21)–C(028)–N(21)	119.4(3)
S(12)–Mo–S(22)	83.02(4)	Mo–S(22)–C(027)	110.3(1)	C(011)–C(016)–C(015)	118.9(5)	S(21)–C(028)–C(027)	119.3(3)
S(12)–Mo–S(32)	81.84(4)	Mo–S(31)–C(038)	110.1(1)	S(12)–C(017)–N(12)	119.3(3)	N(21)–C(028)–C(027)	121.3(4)
S(21)–Mo–S(22)	81.82(4)	Mo–S(32)–C(037)	110.0(2)	S(12)–C(017)–C(018)	119.7(3)	N(31)–C(031)–C(032)	119.3(4)
S(22)–Mo–S(32)	82.12(4)			N(12)–C(017)–C(018)	120.9(4)	N(31)–C(031)–C(036)	120.4(4)
S(31)–Mo–S(32)	81.32(4)	Average Mo–S–C	109.9(3)	S(11)–C(018)–N(11)	118.8(3)	C(032)–C(031)–C(036)	120.2(4)
S(21)–Mo–S(31)	82.16(4)			S(11)–C(018)–C(017)	118.3(3)	C(031)–C(032)–C(033)	120.2(5)
		C(011)–N(11)–C(018)	116.1(4)	N(11)–C(018)–C(017)	122.8(4)	C(032)–C(033)–C(034)	120.6(5)
Average S–Mo–S	81.9(7)	C(016)–N(12)–C(017)	116.6(4)	N(21)–C(021)–C(022)	120.1(4)	C(033)–C(034)–C(035)	120.2(5)
		C(021)–N(21)–C(028)	117.0(4)	N(21)–C(021)–C(026)	121.1(4)	C(034)–C(035)–C(036)	120.0(5)
S(11)–Mo–S(22)	132.02(5)	C(026)–N(22)–C(027)	115.8(4)	C(022)–C(021)–C(026)	118.9(4)	N(32)–C(036)–C(031)	122.8(4)
S(11)–Mo–S(32)	139.20(4)	C(031)–N(31)–C(038)	116.4(4)	C(021)–C(022)–C(023)	122.1(5)	N(32)–C(036)–C(035)	118.4(4)
S(12)–Mo–S(21)	138.68(4)	C(036)–N(32)–C(037)	116.2(4)	C(022)–C(023)–C(024)	119.0(5)	C(031)–C(036)–C(035)	118.7(4)
S(12)–Mo–S(31)	131.63(4)	N(11)–C(011)–C(012)	117.7(5)	C(023)–C(024)–C(025)	119.6(5)	S(32)–C(037)–N(32)	119.7(3)
S(21)–Mo–S(32)	133.18(4)	N(11)–C(011)–C(016)	121.8(4)	C(024)–C(025)–C(026)	122.1(5)	S(32)–C(037)–C(038)	117.8(3)
S(22)–Mo–S(31)	138.21(4)	C(012)–C(011)–C(016)	120.4(5)	N(22)–C(026)–C(021)	122.4(4)	N(32)–C(037)–C(038)	122.4(4)
		C(011)–C(012)–C(013)	118.3(5)	N(22)–C(026)–C(025)	119.3(4)	S(31)–C(038)–N(31)	118.8(3)
Average S–Mo–S	135	C(012)–C(013)–C(014)	120.9(3)	C(021)–C(026)–C(025)	118.3(4)	S(31)–C(038)–C(037)	119.6(3)
		C(013)–C(014)–C(015)	119.6(5)	S(22)–C(027)–N(22)	119.0(3)	N(31)–C(038)–C(037)	121.6(4)

* The numbers in parentheses are estimated standard deviations in the least significant digit.

Table 5. I.r. bands* of qdt complexes of molybdenum(IV)

ν/cm^{-1}		
$[PPh_4]_2[Mo(qdt)_3]\cdot H_2O$	$[Mo(Hqdt)_3]Cl$	Assignment
	3 140w	ν(N–H)
	1 600m	$\nu(NCS)_{asym}$
1 540m	1 540w	
1 360m	1 340m	
1 170s	1 175s	ν(C=C–S)
1 120s	1 120s	$\nu(N–CS)_{sym}$
	1 105s	
	755s	ν(C–S)
760s	650m	skeletal vibrations of ligands
595s	605m	
430m		
405m	405m	
340s	340s	ν(Mo–S)

* Recorded as Nujol mulls between CsI plates.

structure similar to that of $[Mo(mnt)_3]^{2-}$. The observed trigonal prismatic structure for $[Mo(qdt)_3]^{2-}$, therefore, was unexpected and challenges the ideas advanced[19] to explain the adaptation of a non-trigonal prismatic geometry by $[M(mnt)_3]^{2-}$ (M = Mo or W). Further studies are in progress to clarify this situation.

The dimensions of the cation and the ligands in $[PPh_4]_2[Mo(qdt)_3]\cdot H_2O$ are unremarkable. The values of the latter are similar to those found in $[NEt_4]_2[Ni(qdt)_2]\cdot 2H_2O$,[20] with the alternation of C–N and C–C bond lengths within each qdt ligand being consistent with the electronic structure shown in Figure 1 making the predominant contribution to the π-bonding interactions. The anions are linked by H-bonding, *via* the quinoxaline nitrogen atoms through H_2O molecules [N(21) · · · O 3.06 Å]; a similar H-bonding network is found in $[NEt_4]_2[Ni(qdt)_2]\cdot 2H_2O$.[20]

Spectroscopy.—The positions of bands due to the molybdenum complexes in the i.r. spectra of $[PPh_4]_2[Mo(qdt)_3]\cdot H_2O$ and $[Mo(Hqdt)_3]Cl$ are listed in Table 5. The assignments suggested are based on those of Peyronel *et al.*[14] for the vibrations of the free ligand and its Ni complexes.

The u.v.–visible spectrum of $[Mo(qdt)_3]^{2-}$ in solution is dominated by two intense bands with $\lambda_{max.}$ at 396 and 561 nm. On protonation these bands are red-shifted, in the spectrum of $[Mo(Hqdt)_3]Cl$ mulled in Nujol, absorption maxima occur at 450 and 660 nm. $[PPh_4]_2[Mo(qdt)_3]\cdot H_2O$ dissolves in H_2SO_4 (98%) to give a bottle-green solution with absorption maxima close to those of solid $[Mo(Hqdt)_3]Cl$, suggesting that the species present in H_2SO_4 solution is $[Mo(Hqdt)_3]^+$. These u.v.–visible spectroscopic data are summarized in Table 6.

Table 6. U.v.–visible spectroscopic data^a for qdt complexes of molybdenum(IV)

$[PPh_4]_2[Mo(qdt)_3]\cdot H_2O^b$ (in MeCN)	$[PPh_4]_2[Mo(qdt)_3]\cdot H_2O^b$ (in H_2SO_4)	$[Mo(Hqdt)_3]Cl^c$
276 (107)	282 (33.5)	
396 (47)	466 (16.8)	450
561 (55)	681 (26)	660
770 (1.4)		

^{a} $\lambda_{max.}$/nm ($10^{-3}\varepsilon/dm^3\ mol^{-1}\ cm^{-1}$). ^{b} Using cells of path-length 1 mm. ^{c} Recorded as Nujol mull.

Table 7. Hydrogen-1 and ^{13}C n.m.r. chemical shifts^a for H_2qdt and $[Mo(qdt)_3]^{2-}$

Atom^b	H_2qdt	$[Mo(qdt)_3]^{2-}$
$H^{1,4}$	14.25	
$H^{5,8}$	7.4	7.75
$H^{6,7}$	7.28	7.50
$C^{2,3}$	179.3	168.2
$C^{5,8}$	125.5	126.9
$C^{6,7}$	115.6	126.6
$C^{9,10}$	127.9	137.3

^{a} In Me_2SO solution; δ/p.p.m. relative to $SiMe_4$. ^{b} Numbering of quinoxaline skeleton is given in Figure 1.

Table 8. Electrochemical data^a for $[Mo(qdt)_3]$ complexes

Process	Potential^b (V)	Reversibility^c
$[Mo(qdt)_3]^{3-} \rightleftharpoons [Mo(qdt)_3]^{2-}$	−1.70	Reversible
$[Mo(qdt)_3]^{2-} \rightleftharpoons [Mo(qdt)_3]^-$	−0.19	Reversible
$[Mo(qdt)_3]^- \rightleftharpoons [Mo(qdt)_3]^d$	+0.54	Irreversible

^{a} Cyclic voltammograms recorded in MeCN–0.2 mol dm^{-3} $[NBu_4][BF_4]$ at a Pt working electrode. ^{b} Potentials tabulated are $E_{\frac{1}{2}}$ for reversible processes and $E_{p/2}$ (*i.e.* potential at half peak current) for the irreversible process, measured relative to the ferrocene–ferricenium couple at 0.0 V. ^{c} Reversible processes have ΔE_p *ca.* 60 mV and i_{ox}/i_{red} *ca.* 1 at a scan rate of 20 mV s^{-1}. ^{d} The irreversible oxidation is a one-electron process at the Pt electrode but becomes a two-electron process at the same potential at a vitreous carbon electrode.

Protonation of the ligand would be expected to stabilize ligand-based molecular orbitals relative to metal-based molecular orbitals and the bathochromic shift of the intense, low-energy absorptions which accompanies protonation, therefore, suggests that these bands are due to metal-to-ligand charge-transfer transitions.

Hydrogen-1 and ^{13}C n.m.r. spectra have been recorded for $[NEt_4]_2[Mo(qdt)_3]\cdot 3H_2O$ and for H_2qdt; chemical shifts are listed in Table 7. Only one type of ligand structure for $[Mo(qdt)_3]^{2-}$ is detected by n.m.r., as shown by the presence of only two resonances in the ^1H spectrum and four in the ^{13}C spectrum. These n.m.r. results imply that the observed differences of the qdt ligands in the solid state may be due to crystal-packing and/or hydrogen-bonding effects and are not present in solution. Alternatively, slightly different ligand conformations may be rapidly equilibrating in solution.

Electrochemistry.—The electrochemical behaviour of $[Mo(qdt)_3]^{2-}$ in MeCN has been investigated by cyclic voltammetry. The results are summarized in Table 8. The first (reversible) oxidation occurs at a potential at which oxidation should be readily accomplished by chemical oxidants. Thus addition of I_2 to solutions of $[Mo(qdt)_3]^{2-}$ in MeCN (or CH_2Cl_2) produces an olive-green colouration and a Mo^V e.s.r. signal (g = 2.002, $\bar{A}$ = 32.9), consistent with the formation of $[Mo(qdt)_3]^-$. [Pilipenko *et al.*[7] detected an e.s.r. signal at g = 2.004(2) which they attributed to this complex.]

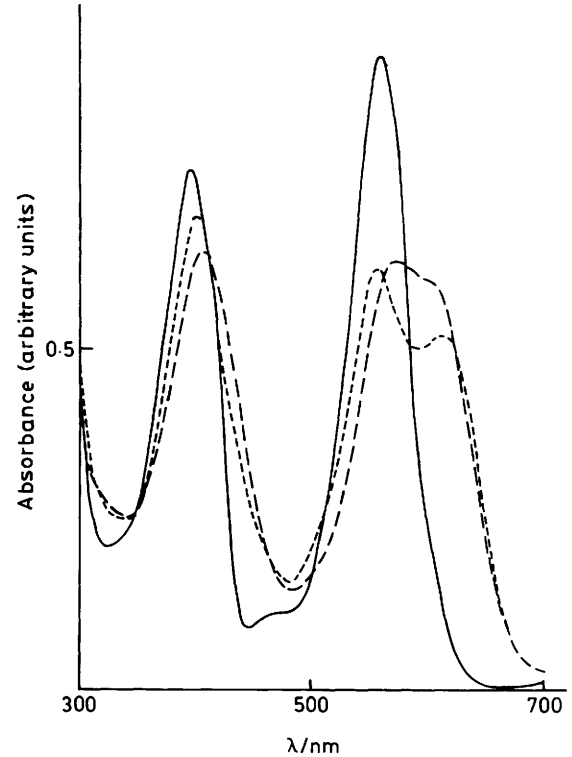

Figure 3. U.v.–visible spectra: 1.7 × 10^{-4} mol dm^{-3} $[Mo(qdt)_3]^{2-}$ in (*i*) dmf (———), (*ii*) toluene-4-sulphonic acid (2.3 × 10^{-3} mol dm^{-3}) in dmf (- - - - -), and (*iii*) toluene-4-sulphonic acid (0.17 mol dm^{-3}) in dmf (— —)

The second oxidation showed no signs of reversibility, even in media less nucleophilic than MeCN, *viz.* CH_2Cl_2 or $[NBu_4][BF_4]\cdot 3PhMe$.[21]

Protonation.—From the presence of a ν(N–H) band in the i.r. spectrum and by analogy with the structurally characterized Ni complexes, $[NEt_4]_2[Ni(qdt)_2]\cdot 2H_2O$[20] and $[Ni(qdt)_2]\cdot dmf$ (dmf = dimethylformamide),[22] it is considered that each of the ligands in $[Mo(Hqdt)_3]Cl$ is singly protonated at a nitrogen atom. Protonation of the ligands renders the complex insoluble in most organic solvents; although $[Mo(Hqdt)_3]Cl$ dissolves in some basic solvents, *e.g.* dmf and Me_2SO, the positions of band maxima in the u.v.–visible spectra of the resulting solutions are intermediate between those of $[Mo(qdt)_3]^{2-}$ (in solution) and $[Mo(Hqdt)_3]^+$ (mulled in Nujol), suggesting that dissolution is accompanied by partial deprotonation. The existence of species in solution intermediate between $[Mo(qdt)_3]^{2-}$ and $[Mo(Hqdt)_3]^+$ {*i.e.* $[Mo(qdt)_2(Hqdt)]^-$ and $[Mo(qdt)(Hqdt)_2]$} is evident from comparison of the u.v.–visible spectra of solutions of $[Mo(qdt)_3]^{2-}$ in dmf, containing different concentrations of toluene-4-sulphonic acid. The u.v.–visible spectra of three such solutions are shown superimposed in Figure 3; the absence of isosbestic points implies that at least three spectroscopically distinct species are present in solution.

The protonation reactions are fully reversible; $[Mo(Hqdt)_3]Cl$ dissolves in solvents containing base, *e.g.* MeCN containing NEt_3 or MeOH containing NaOMe, to give purple solutions from which $[Mo(qdt)_3]^{2-}$ salts can be isolated.

Acknowledgements

We wish to thank the S.E.R.C. for provision of a studentship (to S. B.) and N.A.T.O. for supporting the collaboration between C. D. G. and J. H. E. Financial support by the National Institute of Environmental Health Science (to J. H. E.) is also gratefully acknowledged. The crystal structure was determined in the Molecular Structure Laboratory at the University of Arizona.

References

1 J. L. Johnson and K. V. Rajagopalan, *Proc. Natl. Acad. Sci. USA*, 1982, **79**, 6856; J. L. Johnson, B. E. Hainline, K. V. Rajagopalan, and B. H. Arison, *J. Biol. Chem.*, 1984, **259**, 5414.
2 J. A. McCleverty, *Prog. Inorg. Chem.*, 1969, **10**, 48.
3 A. Pignedoli, G. Peyronel, and W. Malawasi, *J. Inorg. Nucl. Chem.*, 1976, **38**, 1963.
4 L. J. Theriot, K. K. Ganguli, S. Kavarnos, and I. Bernal, *J. Inorg. Nucl. Chem.*, 1969, **31**, 3133.
5 K. K. Ganguli, G. O. Carlisle, H. J. Hu, L. J. Theriot, and I. Bernal, *J. Inorg. Nucl. Chem.*, 1971, **33**, 3579.
6 J. A. W. Dalziel, J. D. Donaldson, B. D. Mehta, and M. J. Tricker, *J. Inorg. Nucl. Chem.*, 1973, **35**, 3811.
7 A. T. Pilipenko, V. V. Trachevskii, and N. V. Rusetskaya, *Russ. J. Inorg. Chem.*, 1979, **24**, 697.
8 A. Furst and D. C. Morrison, *J. Org. Chem.*, 1956, **21**, 470.
9 M. M. Jones, *J. Am. Chem. Soc.*, 1959, **81**, 3188.
10 D. T. Cromer and J. T. Waber, 'International Tables for *X*-Ray Crystallography,' Kynoch Press, Birmingham, 1974, vol. 4, Table 2.2B.
11 J. A. Ibers and W. C. Hamilton, *Acta Crystallogr.*, 1964, **17**, 781.
12 D. T. Cromer and J. T. Waber, 'International Tables for *X*-Ray Crystallography,' Kynoch Press, Birmingham, 1974, vol. 4, Table 2.3.1.
13 B. A. Frenz, 'The Enraf-Nonius CAD 4 SDP-A real-time system for concurrent *X*-ray data collection and crystal structure determination,' in 'Computing in Crystallography,' eds. H. Schenk, R. Olthof-Hazelkamp, H. van Konigsveld, and G. C. Bassi, Delft University Press, Delft, Holland, 1978, pp. 64—71.
14 G. Peyronel, A. Pignedoli, and W. Malawasi, *Spectrochim. Acta, Part A*, 1976, **32**, 1015.
15 T. W. Gilbert, jun., and E. B. Sandell, *J. Am. Chem. Soc.*, 1960, **82**, 1087.
16 M. Cowie and M. J. Bennett, *Inorg. Chem.*, 1976, **15**, 1584.
17 A. E. Smith, G. N. Schrauzer, V. P. Mayweg, and W. Heinrich, *J. Am. Chem. Soc.*, 1965, **87**, 5798.
18 G. F. Brown and E. I. Stiefel, *Chem. Commun.*, 1970, 728.
19 G. F. Brown and E. I. Stiefel, *Inorg. Chem.*, 1973, **12**, 2140.
20 A. Pignedoli, G. Peyronel, and L. Antolini, *Acta Crystallogr., Sect. B*, 1974, **30**, 2181.
21 C. J. Pickett, *J. Chem. Soc., Chem. Commun.*, 1985, 323.
22 A. Pignedoli and G. Peyronel, *Acta Crystallogr., Sect. B*, 1977, **33**, 1439.

Received 2nd January 1986; *Paper* 6/001